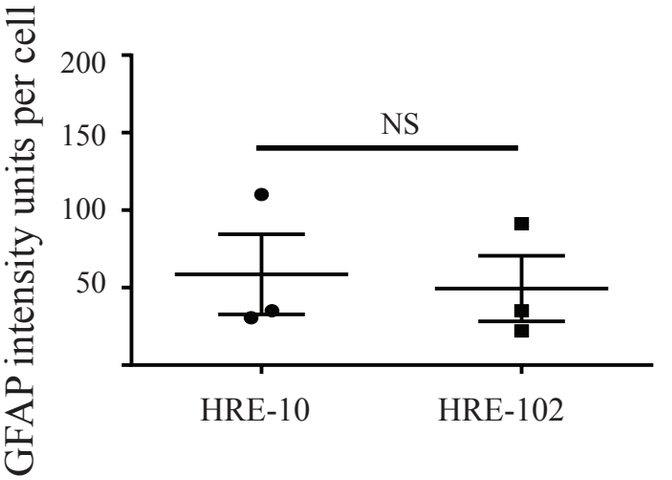

Figure S1. No differences in astrogliosis between HRE-10 and HRE-102 mice. GFAP immunoreactivity in twelve-month cerebellar tissue was similar between HRE-10 and HRE-102 mice (n=3 for each; p=0.79, unpaired two-tailed Student's t-test; mean ± SEM).

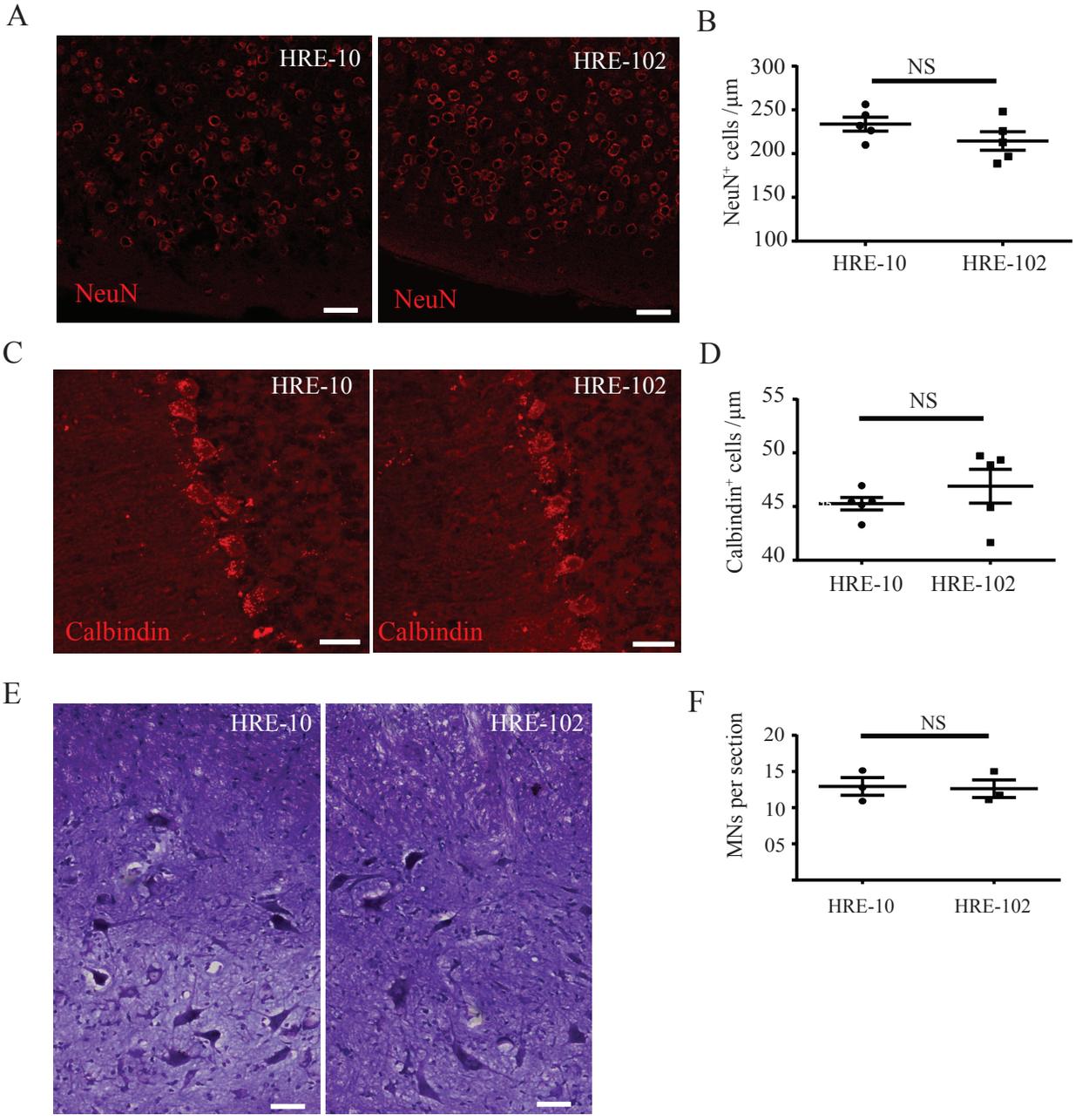

Figure S2. No evidence of loss of neuronal cell bodies in the cortex or cerebellum of HRE-102 mice.
(A) NeuN immunoreactivity in the cortex in twelve-month cortical tissue was not significantly different (B) between repeat expansion mice (n=5 for each; p=0.15, unpaired two-tailed Student's t-test with Welch's correction; mean ± SEM). (C) Calbindin immunoreactivity, used to label Purkinje cells in the cerebellum, was not significantly different (D) between HRE-10 and HRE-102 mice (n=5 for each; p=0.37, unpaired two-tailed Student's t-test with Welch's correction; mean ± SEM). (E) Nissl staining of spinal cord sections show that there are no significant differences (F) between HRE-10 and HRE-102 in the number of motor neurons in the spinal cord (n=3 for each; p=0.87, unpaired two-tailed Student's t-test with Welch's correction; mean ± SEM). Scale bar for (A): 10µm, (C): 20µm, (E): 20 µm.

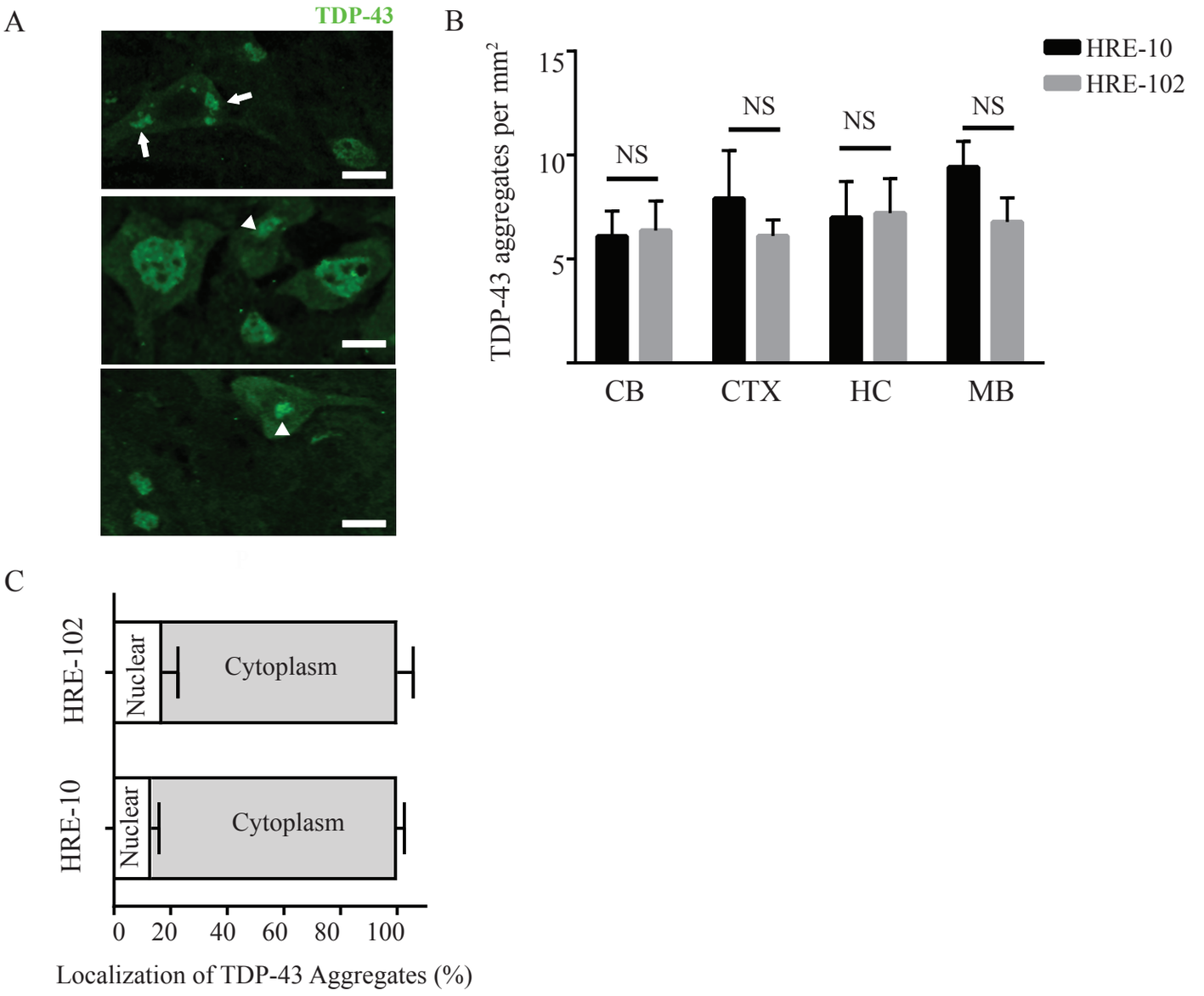

Figure S3. No differences in presence of TDP-43 aggregates between HRE-10 and HRE-102 mice. (A) Infrequent TDP-43 aggregates were identified in the nucleus (arrowhead) and cytoplasm (arrow) of brain tissue in (B) multiple regions, though there were no significant differences detected between the HRE-10 and HRE-102 mice in either the cerebellum (CB, n=3 for each; p=0.89), cortex (CTX, n=6 for each; p=0.48), hippocampus (HC, n=6 for each; p=0.93), or midbrain (MB, n=6 for each; p=0.15). (C) The majority of TDP-43 aggregates in both sets of mice were found in the cytoplasm (HRE-10:n=6, HRE-102:n=5; p=0.87) with a minority in the nucleus (HRE-10: n=6, HRE-102: n=5; p=0.52). An unpaired two-tailed Student's t-test was used to assess data between the two mouse groups for all comparisons. Scale bar for (A): 10µm.

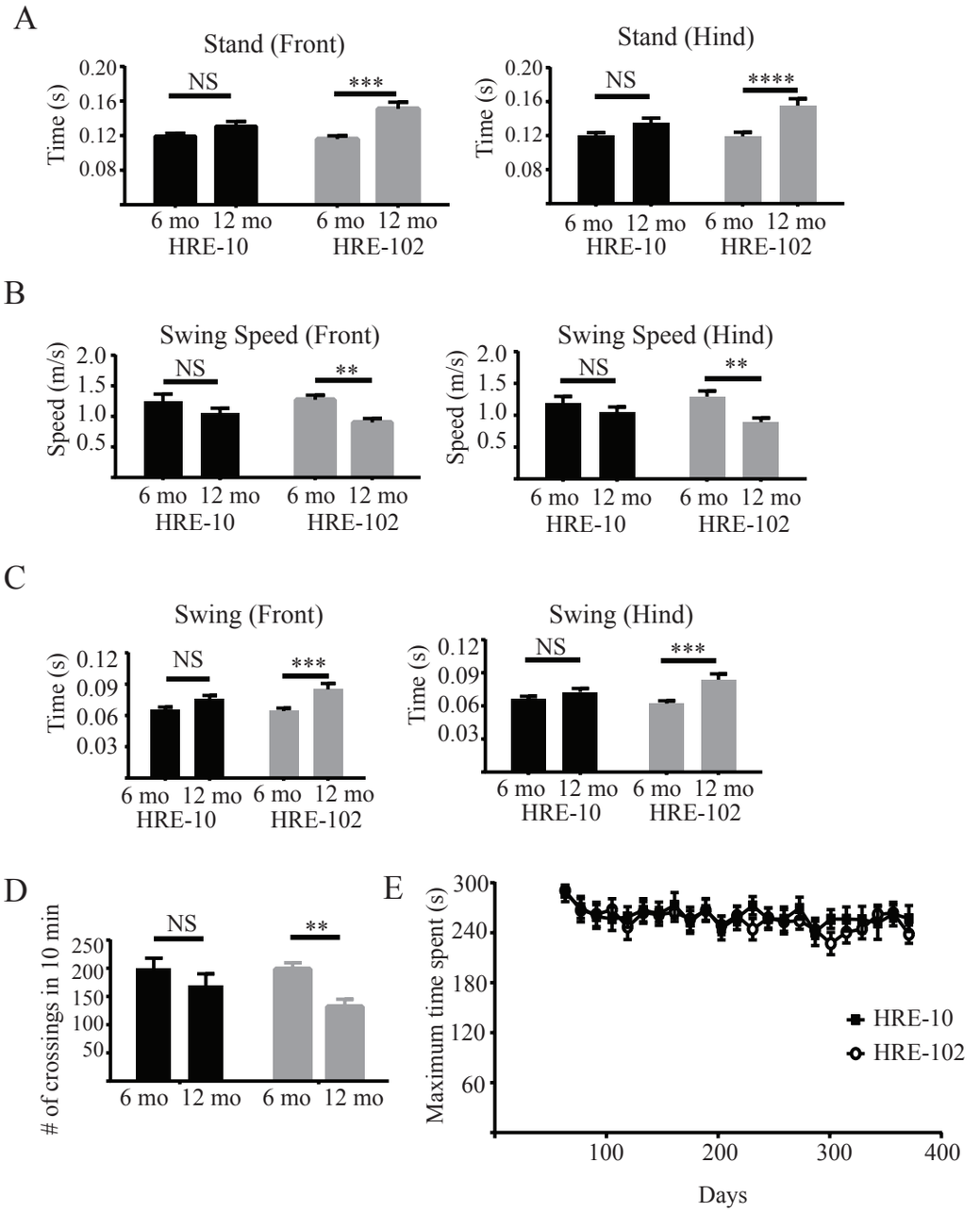

Fig S4. HRE-102 mice show age-related deficits in gait and activity compared to HRE-10 mice. (A-C) Progressive changes in HRE-102 mice in several gait phenotypes such as the front and hind stand index, front and hind swing speed, and front and hind swing are not observed in HRE-10 mice (HRE-10:n=11, HRE-102:n=13; front stand index: [F(1,42)=17.87, ***p=0.0001, post-hoc Sidek: HRE-10 (p=0.29), HRE-102 (p<0.0001)], hind stand index:[F(1,42)=18.63, ****p<0.0001, post-hoc Sidek:HRE-10 (p=0.17), HRE-102 (p=0.0001)], front swing speed:[F(1,42)=10.93, **p=0.002, post-hoc Sidek:HRE-10 (p=0.22), HRE-102 (p=0.007)], hind swing speed:[F(1,42)=9.27, **p=0.004, post-hoc Sidek: HRE-10 (p=0.49), HRE-102 (p=0.004)], front swing:[F(1,42)=15.96, ***p=0.0003, post-hoc Sidek:HRE-10 (p=0.15), HRE-102 (p=0.0007)], hind swing:[F(1,42)=14.46, ***p=0.0005, post-hoc Sidek:HRE-10 (p=0.42), HRE-102 (p=0.0002)]. (D) HRE-102 mice were increasingly hypoactive with age in the open field in contrast to HRE-10 mice (HRE-10:n=10, HRE-102:n=13; front stand index:[F(1,42)=9.69, **p=0.003, post-hoc Sidek: HRE-10 (p=0.36), HRE-102 (p=0.005)]. (E) There were no differences on the accelerating rotarod between HRE-10 and HRE-102 mice [F(22,484)=0.84, p=0.67]; Two-way ANOVA, genotype x age interaction, all data presented as mean ± SEM.